Effective Vs and Vp characterization from Surface Waves streamer data along river embankments

Effective Vs and Vp characterization from Surface Waves streamer data along river embankments.

Comina C.[1], Vagnon F.[1], Arato A.[2], Antonietti A.[2]
[1]Dipartimento di Scienze della Terra, Università degli studi di Torino, Torino (IT)
[2] Techgea S.r.l., Torino (IT).

ABSTRACT

River embankments are linearly extended earth structures built for river flood protection. Their continuity and uniformity are fundamental prerequisites to ensure and maintain their protection efficiency. Weakness points usually develop in localized areas where geotechnical variability is present in the embankment body or in the underlying subsoil. Given their significant length, and the localized nature of weakness points, the characterization of river embankments cannot therefore rely on local geotechnical investigations but requires the application of efficient and economically affordable methods, able to investigate relevant lengths in a profitable way. This is even more essential when the investigations are conducted near, or in foresee of, significant flood events, when timing of the surveys is essential. In this paper the application of a procedure (W/D procedure) for the seismic characterization of river embankments, specifically designed for surface waves streamer data, is presented. The W/D procedure allows the combined definition of 2D shear (Vs) and compressional (Vp) wave velocity models and can be developed in order to be automated as a fast imaging tool. Its application to the characterization of a test site (Bormida river embankment, Piedmont Region, Italy) is presented. It is also shown that the obtained results are comparable to standard seismic processing approaches with the advantage of reduced survey time and increased efficiency, giving preliminary results directly in the field.

Article Highlights:

- Effective Vs and Vp information are extracted from surface waves streamer data**;**
- An automated procedure for the seismic characterization of river embankments was developed;
- The procedure is demonstrated comparable to standard seismic processing approaches;
- Advantages in survey time and efficiency is highlighted.

Keywords: surface waves, seismic characterization, river embankments.

Corresponding author: Cesare Comina, cesare.comina@unito.it

1. INTRODUCTION

River embankments are linearly extended earth structures constructed to serve as flood control systems during large rain events. A proper characterization of the embankment body is essential to verify its uniformity and to monitor the occurrence of possible integrity losses which could undermine its stability. In recent years, frequency and magnitude of extreme flood events have been rapidly increasing in Central America, Southern Europe, and in Italy because of climate change. Moreover, the poor maintenance of hydraulic structures, mostly reaching their design service life, makes the adoption of specific interventions of paramount international relevance.

Given the significant length extension of these structures, and the localized nature of weakness points, the characterization cannot rely only on local geotechnical investigations but requires the application of efficient and economically affordable methods, able to investigate the whole embankments in a profitable way. Moreover, geotechnical investigations usually require invasive procedures (such as boreholes, penetration tests, etc) that are both expensive and time-consuming. With this respect non-invasive, rapid and cost-effective methods are desirable to identify higher potential hazard zones.

Among the available non-invasive geophysical methods (Chao et al., 2006; Bergamo et al., 2016; Takahashi et al., 2014; Sentenac et al., 2018), the seismic ones have peculiar advantages for the soil characterization. Seismic velocities, and particularly shear wave velocity (Vs), are directly related to the dynamic stiffness of the material, which is an important mechanical parameter for the recognition of soil layers. Moreover, in the field of geotechnical engineering, huge research effort has been spent on the correlation of Vs to parameters obtained from standard geotechnical tests. Site specific and general correlations exist to porosity, plasticity index, to the shear modulus at higher strains and to standard geotechnical in situ tests such as cone penetration, standard penetration and dilatometer tests (e.g. Kramer, 1996; Samui, 2010; Foti et al., 20014).

Among the seismic methods the multichannel analysis of surface waves (MASW), based on the Rayleigh wave dispersion curve (DC) analysis, is considered the most effective for the determination of Vs profiles. This method can be efficiently applied to seismic streamer data dragged along embankments and overall linear earth structures. This allows the determination of several Vs profiles to offer an almost 2D representation of the velocity field. Several literature applications of this methodology are available along embankments, river dykes and earth dams (e.g. Lutz et al., 2011; Lane et al., 2008; Min and Kim, 2006). Eventually, MASW surveys can be used in combination with geoelectrical and geotechnical methods to allow for more complete characterization (e.g. Samyn et al., 2014; Busato et al., 2016; Bièvre et al., 2017; Rahimi et al., 2018; Arato et al. 2020).

The main limitations of this methodology are related to the high non-linearity of the DC inversion procedure and to the lack of compressional wave velocity (Vp) information. Several global inversion approaches have been proposed for the DC inversion (e.g. Socco and Boiero, 2008), with the aim of tackling the problem of non-uniqueness of the solution. More elaborated inversion strategies for reconstructing 2D shear wave velocity sections including waveform information (e.g. wave-equation dispersion inversion (WD), Li et al., 2017, or multi-objective waveform inversion (MOWI), Pan et al., 2020) have been also proposed. Nevertheless, all these approaches are highly time consuming, particularly for increasing number of DCs to be analysed, and can be adopted only in the post-processing stage, not allowing for an effective in situ characterization. The lack of Vp information can also be a disadvantage since Vp is known to be correlated with saturation levels and related Poisson ratio of the materials. This last could be indeed an important parameter to be determined along river embankments, to complete the characterization.

To overcome these limitations, the application of a new procedure (Socco et al., 2017; Socco and Comina, 2017) for the analysis of Rayleigh wave fundamental mode DC is adopted in this paper. This procedure is based on the relationship between Rayleigh wave wavelength and investigation depth (W/D procedure) and exploit the higher sensitivity of the DCs to time-average shear wave velocity (Vs,z) than to layered velocity profiles and the sensitivity of the Rayleigh wave skin depth to Vp. The W/D procedure allows the determination of both 2D Vs and Vp sections from the DCs using a direct data transform approach. The relationship between the wavelength of the Rayleigh wave fundamental mode and the investigation depth (W/D relationship) is estimated through a reference Vs and Vs,z profile and used to directly transform all DCs into Vs profiles. The sensitivity of the W/D relationship to Poisson ratio is moreover exploited to obtain also Vp profiles along the studied embankment. The procedure has already demonstrated its reliability both on synthetic and real data, producing Vs and Vp models which allow a reliable waveform matching in comparison to benchmarks (Khosro Anjom et al., 2019) and effective full waveform inversion starting models (Teodor et al., 2020).

Another significant advantage of the proposed W/D procedure is that, being a data transform approach, it does not have particular computational requirements. In principle, it could therefore be applied also during in situ measurement campaigns for a fast imaging of the seismic properties of the studied embankment. This products a strong reduction of survey time and increased efficiency. In this paper, the procedure is specifically implemented for surface waves streamer data and its application to the characterization of a test site (Bormida river embankment, Piedmont Region, Italy) is presented. It is shown that the obtained results are comparable to standard seismic

processing approaches with the advantage of reduced survey time and increased efficiency, and that preliminary results can be obtained directly during in situ measurements.

2. TEST SITE AND EXECUTED SURVEYS

The test site investigated in this paper is the right embankment of the Bormida river, east of the city of Alessandria, in Spinetta Marengo municipality, Piedmont Region, NW Italy (Figure 1). The embankment is separated from the river by the presence of a 200 m wide floodplain that serves as expansion area during floods (Figure 1). The top of the embankment rises about 9 m from the free surface of the river, and about 3 m from the floodplain. The soil composition of the embankment (embankment body and foundation) was obtained by available geotechnical tests: a borehole, executed on the top of the embankment in correspondence of an embankment curve (S1, in Figure 1 inlet) and a dynamic penetration super heavy test (DPSH) executed in the proximity of the borehole. Both the borehole and DPSH interested embankment body and foundation soil till about 16 m depth.

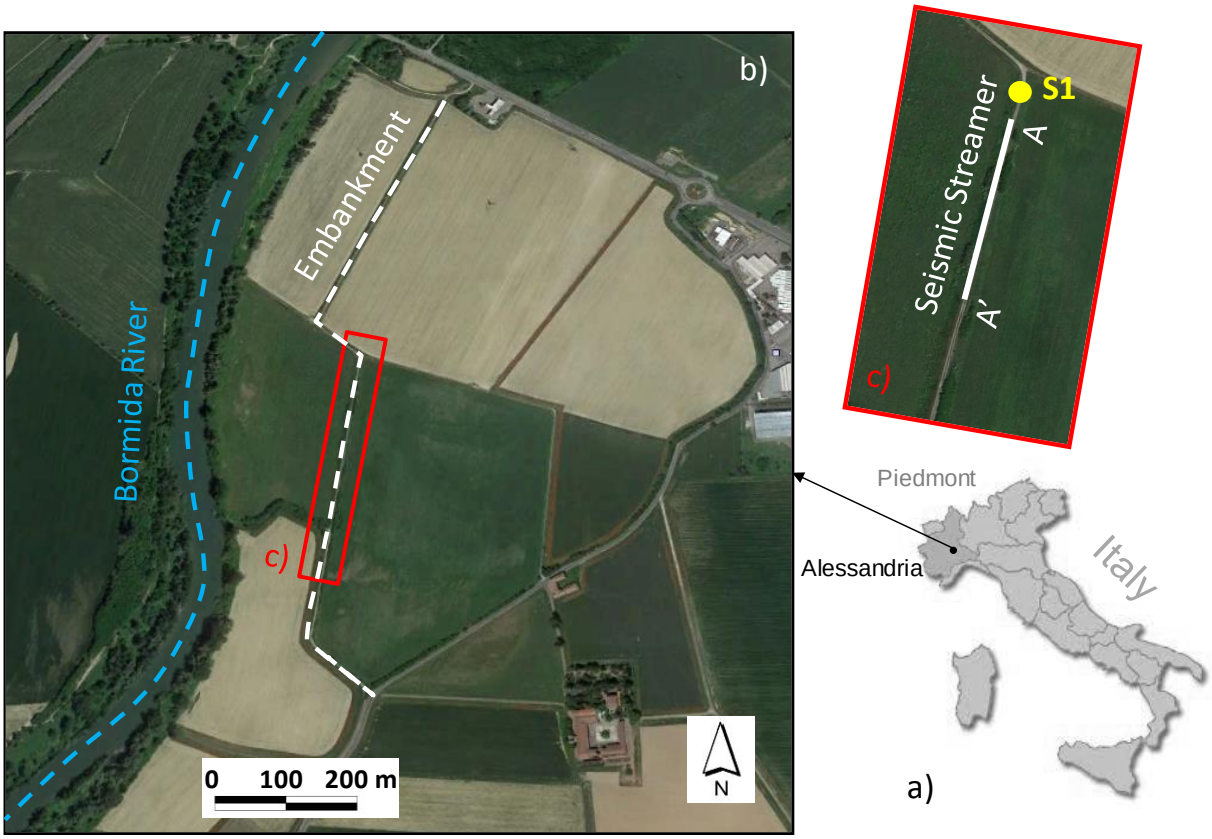

Figure 1 – Location of the test site: a) north western Italian Po plain, Piedmont region, near the city of Alessandria, b) detail of the studied embankment and c) executed surveys.

The geotechnical setting (Figure 2) can be synthetized as constituted by silts with fine sands and scattered clasts changing to fine to medium grained sands, moderately compacted, with sporadic

clasts, up to about 5.3 m depth (embankment body) overlaying a coarse sand and gravel formation moderately to medium compacted with intercalated silts and local compaction reduction with depth. At the moment of execution of the borehole (November 2007) the water table was reported at about 10 m depth from the embankment top; given the height of the river, the water table is therefore supposed to be fed by the river and its elevation strictly dependent on the water level within the river.

As it can be observed in the stratigraphic log, the transition from embankment body to natural subsoil does not appear to be particularly sharp. This can be an indication that the construction procedure did not involved relevant reworking of the first subsoil and that lateral differences in depth and nature of this contact could be present along the embankment. Taking as reference the DPSH result, local eventual differences along the embankment body will be investigated using seismic streamer data dragged along a specific portion of the embankment (Figure 1).

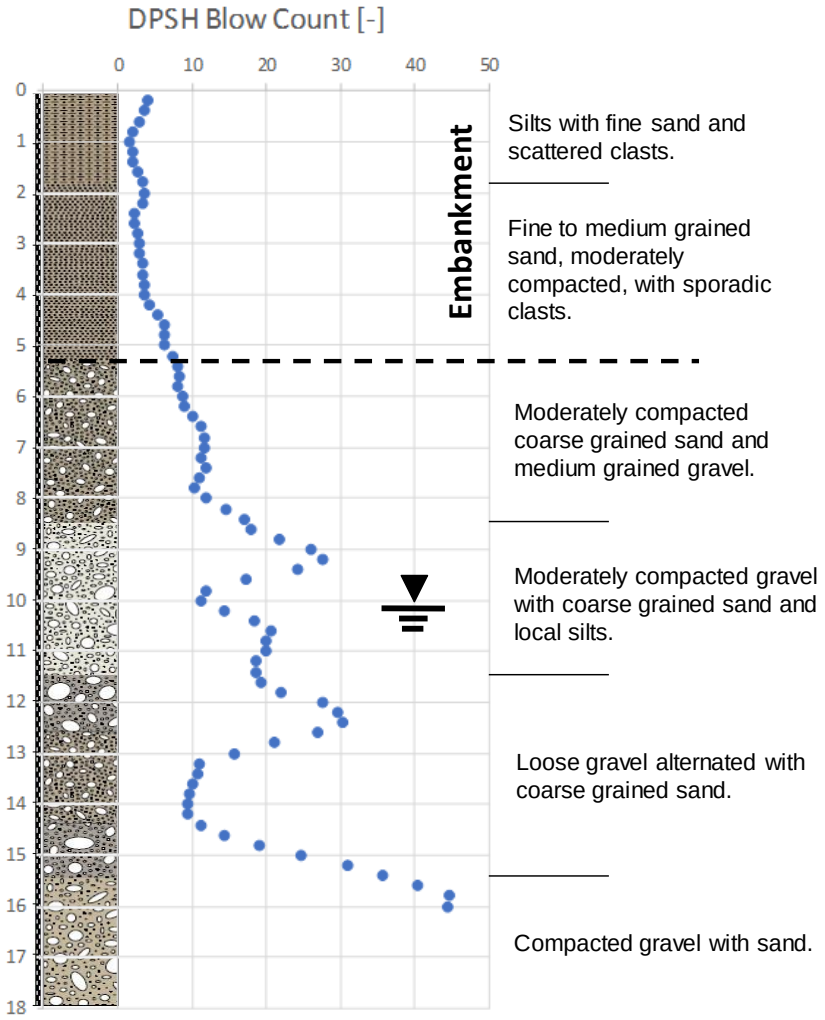

Figure 2 – Stratigraphic log and geotechnical description of the encountered formations with evidence of the DPSH results.

An embankment sector of about 90 m, south with respect to the S1 borehole (Figure 1), was investigated in May 2019 with a seismic land streamer constituted of 24, 4.5 Hz vertical geophones mounted on coupling sliders at 1 m spacing. The streamer was dragged by a pick-up truck and was moved along the studied reach at 2 m steps; for each moving step a single seismic shot was registered. The seismic source was a 40 kg accelerated mass mounted on the pick-up back; a 5 m source offset was adopted in the acquisitions. The streamer was connected to a DaQLink IV (Seismic Source, 2016) acquisition device on the pick-up truck, storing the data in a survey laptop and eventually applying pre-processing steps. Seismograms where acquired with a 0.5 ms sampling interval, -50 ms pretrig and 1.024 s total recording length. A total of 45 seismograms were therefore acquired during the survey. On these data several processing steps were applied for the definition of 2D Vs and Vp models with the proposed W/D procedure.

3. METHODOLOGY

An example seismic shot is reported in Figure 3a. The used source and streamer setup allowed the acquisition of high-quality data, with clear evidence of surface waves dispersive pattern and also particularly evident first arrivals of compressional waves.

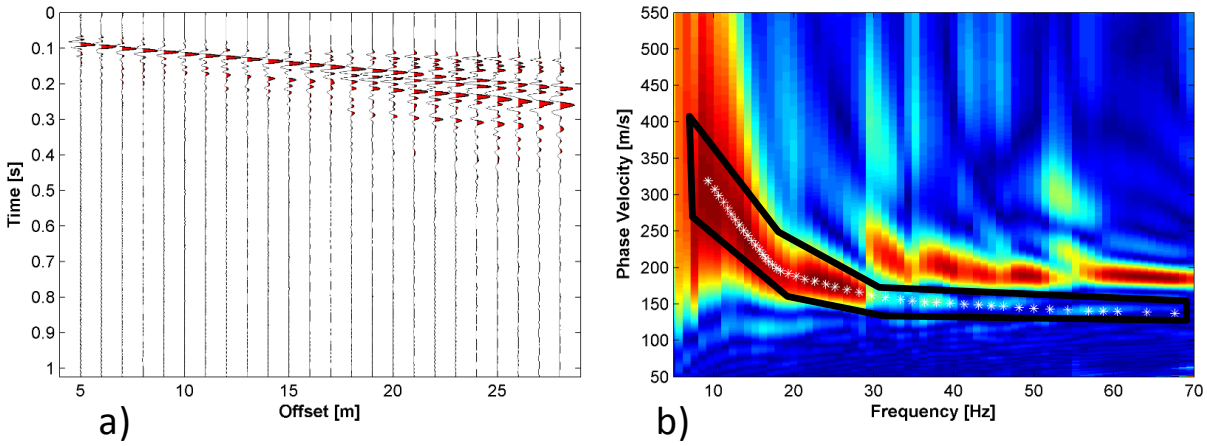

Figure 3 – Data processing procedures on acquired seismograms: a) example seismic shot, b) dispersion curve extraction with evidence of the applied mask (black line) and selected high energy maxima (white asterisks).

DCs extraction was performed with two different procedures: first, the dispersion image for each seismogram was obtained by means of a phase-shift approach (Park et al., 1998) implemented in MATLAB® routines. The phase-shift approach has demonstrated to maintain very good performances even when a limited number of traces is considered (Dal Moro et al., 2005). Alternatively, to further improve the accuracy of dispersion measurement, a multi-channel

nonlinear signal comparison (MNLSC, Hu et al., 2019) can be adopted, producing high and adjustable resolution among a wide detected frequency range.

On the dispersion image the zone pertinent to the fundamental mode propagation was selected with a mask (black line in Figure 3b) and energy maxima were automatically searched within this area (white asterisks in Figure 3b). The mask selected for the first shot can be either automatically used for all the following shots (automatic procedure) or partially adjusted to follow eventual variations in the energy distribution (semi-automatic procedure). In the first case a rough, but fully automated, DCs selection is obtained, in the second case a more refined, but more time consuming, analysis is allowed, to better evidence eventual lateral variations. On both these selected DC groups eventual smoothing and manual outlier removal can be applied to obtain more continuous and reliable curves.

In Figure 4 the resulting DCs selected for all the shots from automatic and semi-automatic procedures are reported. For some of the shots a transition of the absolute energy maxima towards higher modes was observed in the high-frequency range (e.g. frequencies higher than 30Hz in Figure 3b). Nevertheless the fundamental mode can still be followed as local maxima thank to the adopted mask that allowed to isolate the correct portion of the dispersion image to be considered, excluding the higher modes from the maxima searching. It can be evidenced that the DC ranges are very similar with corresponding velocity transition. Nevertheless, the semi-automatic procedure (Figure 4b) shows higher variability for the medium-high frequency range (shallower layers) as a result of the application of a variable mask. Most of the results reported in the paper refer to the DCs selected with this approach. In the discussion section some comparisons are however presented with the results obtainable with the automatic procedure also.

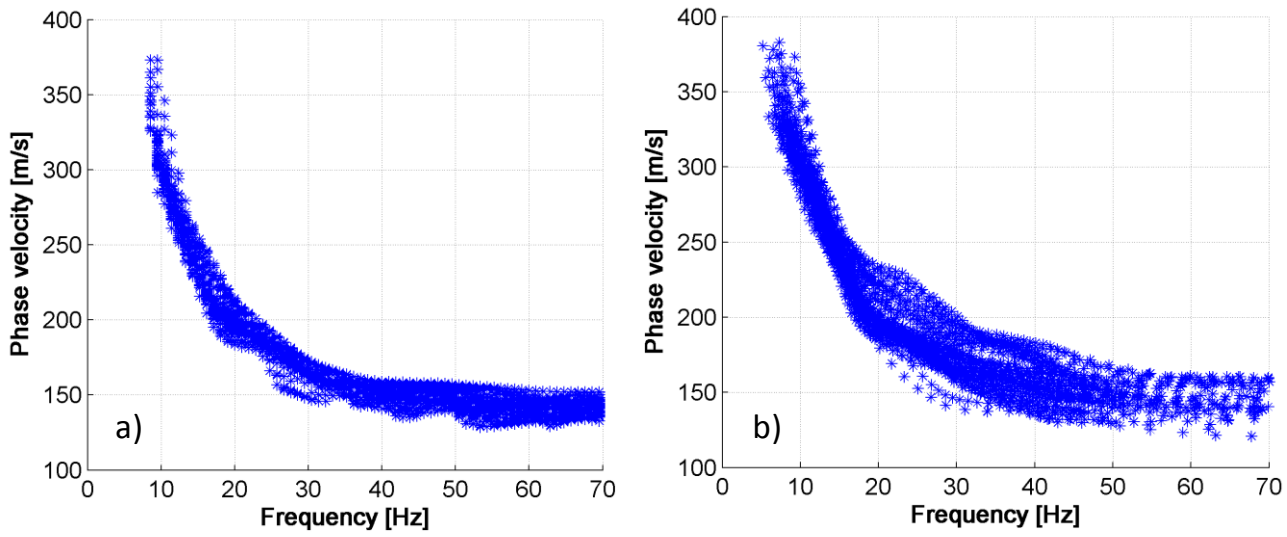

Figure 4 – DCs selected for all the shots: a) automatic procedure and b) semi-automatic procedure.

188 The application of the W/D procedure to the extracted DCs requires the knowledge of a single Vs
189 and Vs,z reference profile along the seismic line together with its associated DC. This profile can be
190 either extracted from the data themselves, by performing the inversion of a representative DC
191 among the ones extracted, or it can be obtained by independent seismic or geotechnical data.
192 In this paper the first method was adopted using a Monte Carlo Inversion (MCI) algorithm (Socco
193 and Boiero, 2008) which efficiently limits potential non-uniqueness of the solution and results in
194 reliable Vs and Vs,z profiles. The inversion implies the definition of a wide model space by
195 selecting ranges for each model parameter (Vs, thicknesses and the Poisson ratio of each layer) and
196 performing random sampling (10^5 profiles) among these ranges. Please note that, in order to allow
197 for the W/D procedure to be applied, also Poisson ratio of each layer is considered as a model
198 parameter, contrary to what usually performed in the inversion of DC curves.
199 Example application of the inversion process to the DC reported in Figure 3b, which was selected
200 as reference, is reported in Figure 5. It can be observed that the set of statistical equivalent profiles
201 selected from the MCI assess the presence of a contrast at the bottom of the embankment around 5
202 m depth (Figure 5b). This set of profiles, and their correspondent numerical DCs, is represented in
203 Figure 5 with a relative misfit representation based on the absolute difference between each profile
204 misfit and the best fitting one (in red in Figure 5).
205 It can also be noted that the higher variability in terms of Vs profiles (Figure 5b) strongly reduces
206 when the time average shear wave velocity is considered (Vs,z, in Figure 5c). With this respect the
207 best selected profile (in red in Figure 5c) and the mean of the statistical set (in black in Figure 5c)
208 almost superimpose for the top portion of the profile. Socco and Comina (2015) have already shown
209 that the non-uniqueness of the DC inversion very slightly affects the estimation of time-average
210 velocity, and hence, the Vs,z obtained from inverted profiles is very robust. Nevertheless, given the
211 increased uncertainty at the bottom of the profile, the following analyses were limited to 20 m
212 depth, which is enough for investigating both the embankment and a significant portion of the
213 foundation subsoil at the studied test site.
214 Using the reference Vs and Vs,z profiles and all the extracted DCs, the proposed data transform
215 procedure is then applied as following: i) the estimated Vs,z and its corresponding DC are used to
216 compute the reference W/D relationship; ii) the reference W/D relationship is used to transform all
217 DCs into Vs,z models; iii) an apparent Poisson ratio is estimated using the reference W/D
218 relationship and the reference Vs model; iv) using the apparent Poisson ratio, each Vs,z profile is
219 transformed into a Vp,z profile; v) all the reconstructed Vs,z and Vp,z profiles are transformed into
220 Vs and Vp profiles with an interval velocity analysis.
221

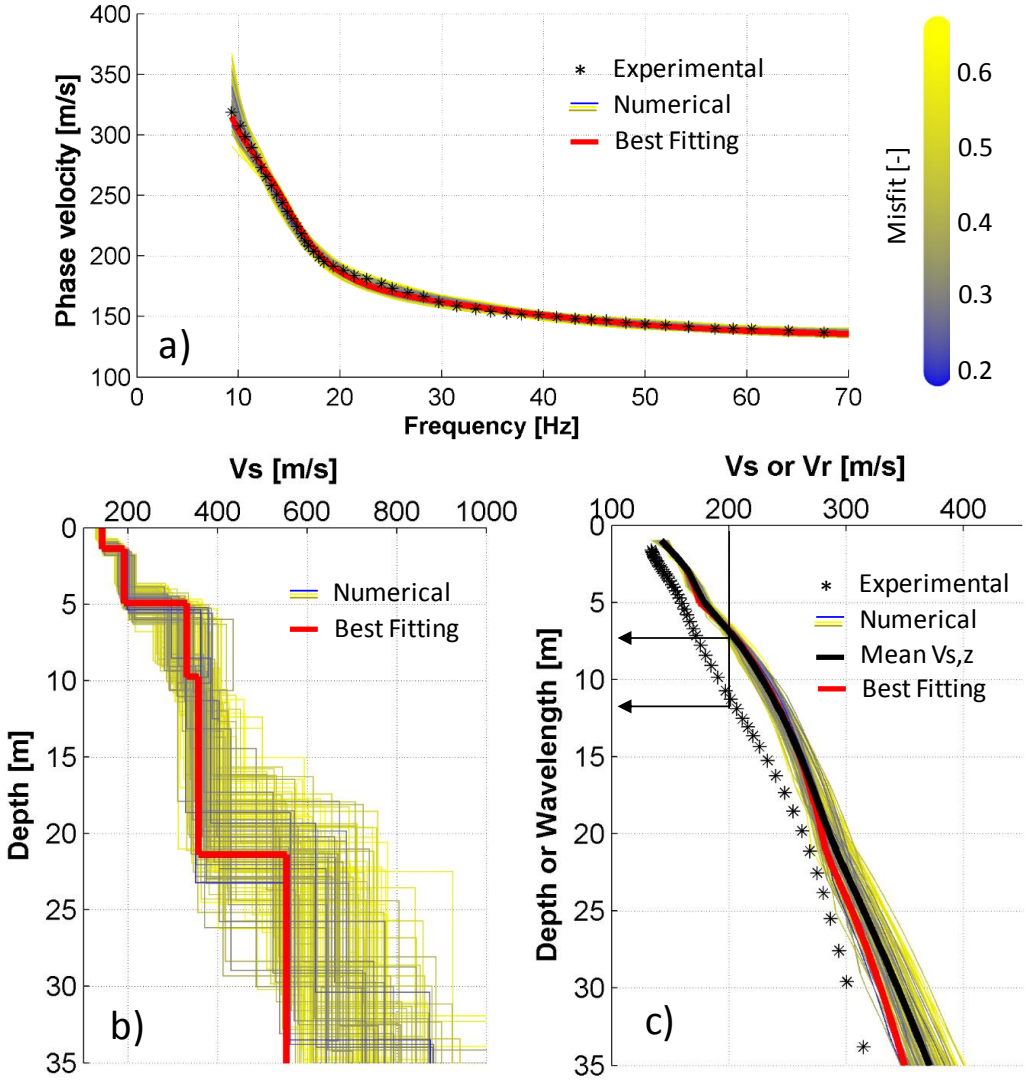

Figure 5 – MCI of the reference DC curve: a) experimental and numerical dispersion curves b) best fitting profile and set of statistically equivalent profiles and c) experimental dispersion curve as a function of wavelength, time average velocities of best fitting profile and statistically equivalent profiles with their mean.

Steps i) and iii) of the procedure require more explanations. The meaning of the W/D relationship is represented in Figure 5c: for each Vs,z value, the wavelength (W) at which the phase velocity (Vr) of the DC is equal to the Vs,z (see the arrows in Figure 5c) is searched for each depth (D). With all the W/D pairs at which Vs,z and phase velocity are equal a relationship is obtained (W/D relationship. This relationship is represented in Figure 6 for the best fitting profile (in red), for the mean of the statistically equivalent profiles (in black) and for all the statistically equivalent profiles. Consistency of the extracted W/D relationships is evidenced.

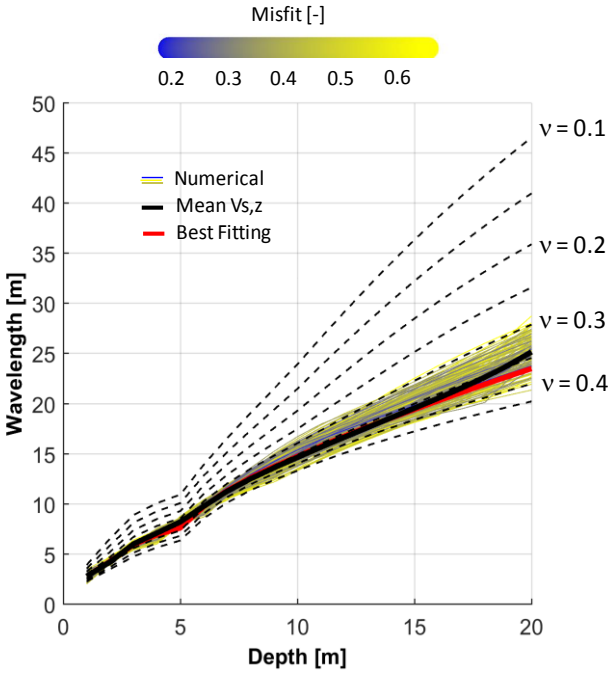

234

235 **Figure 6 – The W/D relationship for the reference DC for the best fitting profile (in red), for the mean**
236 **of the statistically equivalent profiles (in black) and for all the statistically equivalent profiles**
237 **compared with the ones obtained with different Poisson ratio values. Reference Poisson ratio values**
238 **are indicated on the right of the plot.**

239 This relationship represents the surface waves' skin depth for increasing wavelengths and has been
240 demonstrated (Socco and Comina, 2017) to be influenced by the Poisson ratio of the formation.
241 With the reference Vs and Vs,z profiles it is therefore possible to build different synthetic W/D
242 relationships by changing the value of the Poisson ratio (ν) of the layers (assumed constant for all
243 the layers). These synthetic W/D relationships are reported in Figure 6 (dashed black lines) for
244 some example values of the Poisson ratio. It can be noted that Poisson ratio acts on the slope of
245 W/D relationship. In particular, the slope decreases when Poisson ratio increases. Therefore the
246 slope of the experimentally determined W/D relationship contains information on the actual Poisson
247 ratio of the formation. The actual apparent Poisson ratio profile of the formation can be therefore
248 searched by associating to each depth the value of Poisson ratio that corresponds to the linear
249 interpolation between the upper and lower nearest synthetic W/D relationships. In this way an
250 apparent Poisson ratio profile with depth can be obtained for the reference DC. This profile can be
251 later used to transform all the Vs,z profiles into Vp,z profiles allowing for a 2D Vp section to be
252 later computed.
253 An example application of the W/D procedure to the reference DC is reported in Figure 7. It can be
254 observed that the Vs,z of the best fitting profile (continuous red line in Figure 7) and the mean Vs,z
255 of the statistical set (continuous black line in Figure 7) almost superimpose for the first 20 m depth.

It can be also noted that the W/D procedure allows the estimate of a Vs model (in blue in Figure 7) very near to the best fitting one (layered red line in Figure 7) obtained from the MCI of the DC. The model obtained with this procedure has also the advantage of not making any assumption with respect to the number of layers of the profile. For this reason, it can result smoother with respect to the layered profile but also more correspondent to the actual geotechnical situation below the embankment. Particularly, it can be observed that the transition from embankment body to bottom layers with this estimated profile appear to be more correspondent to what evidenced in the DPSH results (Figure 2) with respect to the sharp interface evidenced by the MCI result.

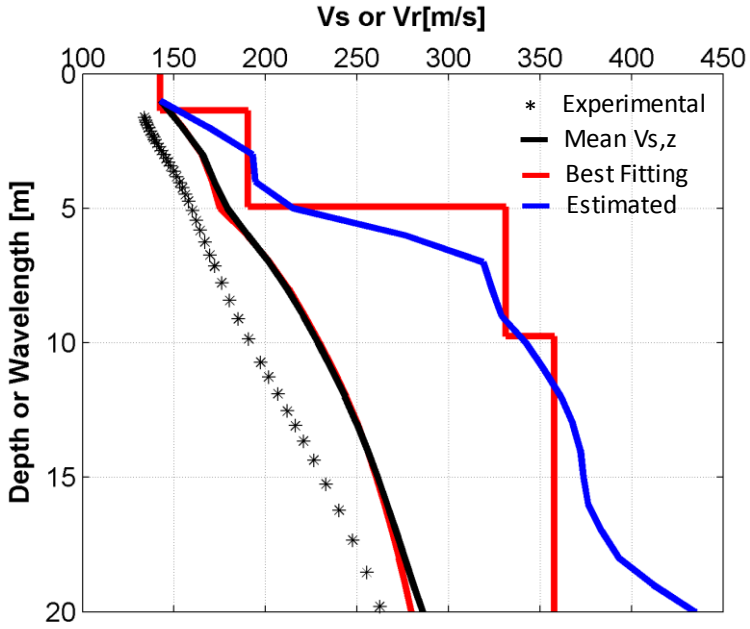

Figure 7 – Application of the W/D procedure to the reference DC for Vs profile determination and comparison with the best fitting result (both in term of layered velocity model and Vs,z) from MCI.

All the Vs and Vp profiles estimated with the W/D procedure are then interpolated along the studied embankment to allow for a 2D visualization of the Vs and Vp velocities distributions. The data gridding was performed in Surfer (Golden software) with an interpolation grid of 2 m in the horizontal direction (equal to the acquisition step) and of 0.5 m in the vertical direction.

To validate the velocity models obtained with the application of the W/D procedure the obtained results are benchmarked against standard seismic processing approaches. For Vs, all the dispersion curves extracted were inverted with a laterally constrained inversion (LCI) approach (Auken and Christiansen, 2004; Socco et al., 2009). For this inversion, the same number of layers of the MCI was assumed. For Vp, processing was carried out by picking the first breaks on each acquired seismogram, picked first breaks were then interpreted in tomographic approach with the use of the software Rayfract (Intelligent Resources Softwares Inc.).

4. RESULTS

Results of the application of the W/D procedure are reported in Figure 8. Particularly, the Vp result is obtained from the Vs one with the application of the apparent Poisson ratio obtained from the W/D procedure. This last is assumed constant through the whole profile and therefore the resulting Vp velocity field is a transformation of the Vs one with similar properties. Both Vs and Vp sections can discriminate the transition from the shallow silts and sands to the bottom gravels along the embankment and delineate the embankment bottom. Coherently with the borehole results and geotechnical tests this transition falls, on the left side of the sections, where the surveys are nearer to the geotechnical tests (the DPSH Blow Count profile is also reported in Figure 8a and b), around 5.3 m depth.

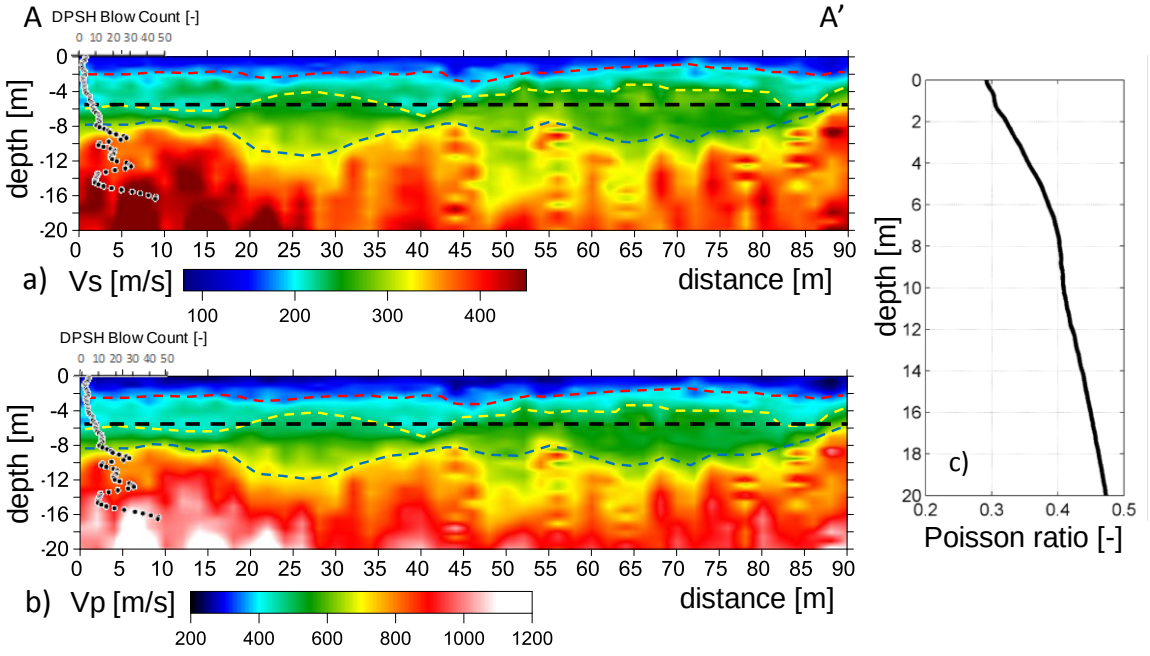

Figure 8 – Results of the application of the W/D procedure to extracted DCs (section A-A'): a) Vs section, b) Vp section (colorbars below each figure) and c) resulting Poisson ratio. On both the sections the supposed depth of the embankment is also reported (dashed black line) together with coloured dashed lines, derived by the velocity models, indicating the transition between the shallow silts and sands (in red), the thickness of the embankment (in yellow) and the transition to compacted gravels and sands (in blue). The DPSH Blow Count profile is also reported at the beginning of the sections.

However, along the embankment a variation of the depth of this interface can be evidenced. Particularly, localized anomalies appear in the Vs section suggesting an increase in the depth of the shallow silts and sands of the embankment (yellow dashed line in Figure 8) around 40 m progressive distance. Conversely, the depth of the interface appears to be shallower in the progressive distance range between about 50 to 80 m.

Seismic surveys are also able to depict the transition (red dashed line in Figure 8) from silts with fine sands and scattered clasts to fine to medium grained sands, as reported from the borehole and DPSH results, within the embankment. A deeper increase in velocity is also observed around 8 m depth on the left side of Figure 8, were the transition to more compacted gravels (blue dashed line in Figure 8) is evidenced by borehole and DPSH results . This more compacted formation appears however to increase its depth along the section moving away from the borehole and showing on average lower velocity values. Localized velocity inversions are also partially observable below 8 m in the leftmost portions of the Vs section. This evidence again well compares with what reported by the DPSH results.

Notwithstanding the information on the position of the water table at the site (around 10 m) the range of Vp velocities extracted by the procedure does not report, for increasing depths, velocity ranges usually attributed to saturated materials (i.e. around 1400-1500 m/s). It must be underlined that the time span between the two surveys is relevant (from November 2007 to May 2019) so that eventual variations on the water table depth could be present. Nevertheless, the Poisson ratio profile extracted with the W/D procedure (Figure 8c) shows a marked increase nearly around 10 m exceeding the 0.4 value and tending to 0.5. Poisson ratio of saturated soils is usually reported to be in this range (Boore, 2007). It must be underlined that the Poisson ratio profile here presented is the interval Poisson ratio obtained through the Vp/Vs ratio of the resulting models. This is different from the apparent Poisson ratio that is estimated in the W/D procedure (Figure 6) for the DC transformation.

Results of the LCI processing of the extracted dispersion curves are reported in Figure 9a. A good convergence of the inversion was obtained with LCI resulting in a final RMS error of 1.7%.

The comparison of the LCI result with the W/D procedure is performed in Figure 9b in term of normalized differences, taking as reference the LCI results, with the formula:

$$ND = \frac{V_{i,LCI} - V_{i,WD}}{V_{i,LCI}} \quad (1)$$

were V_{iWD} is the velocity value obtained from the W/D procedure and V_{iLCI} is the velocity value obtained from the LCI in each location within the models. Therefore, positive values of the normalized difference indicate zones where the W/D procedure underestimate the velocity, negative values indicate the opposite. To allow computing the normalized differences in each point of the models also layered LCI results were gridded with the same interpolation scheme of the W/D procedure results.

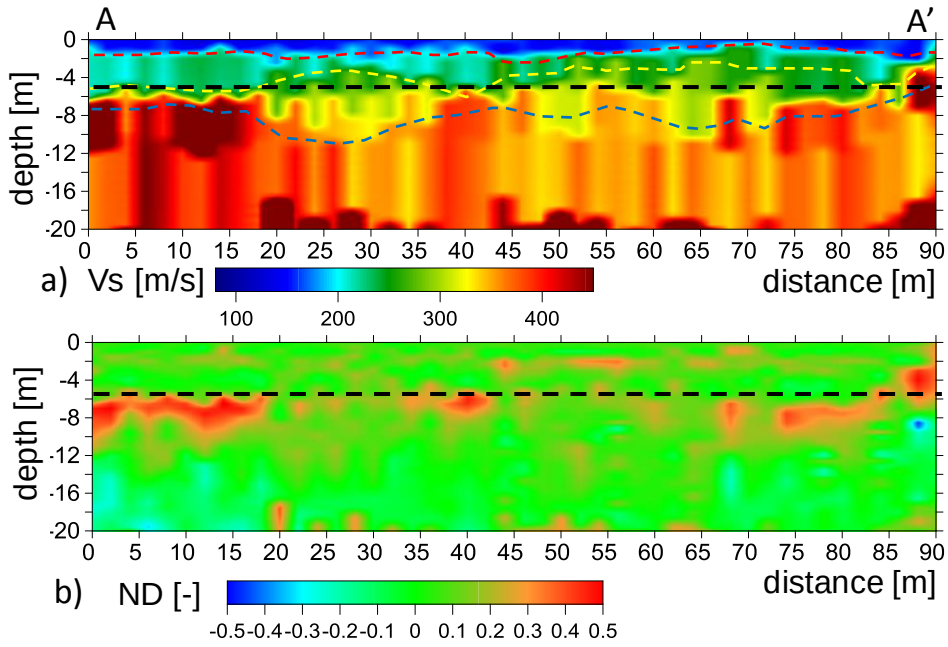

Figure 9 – Results of the LCI of the extracted DCs (section A-A'): a) Vs section and b) Normalized differences with the Vs results of the W/D procedure (colorbars below each figure). On both the sections the supposed depth of the embankment is also reported (dashed black line). Over the LCI section, the interfaces evidenced by the W/D procedure indicating the transition between the shallow silts and sands (in red), the thickness of the embankment (in yellow) and the transition to compacted gravels and sands (in blue), are superimposed.

Figure 9 shows that the Vs velocity range obtained using LCI inversion is comparable with that from the W/D procedure. The interfaces evidenced by the W/D procedure are reported for comparison over the resulting Vs image. Similar variability in the depth of the interfaces is noted. As an example, both the increased depth of shallower silts and sands around progressive 40 m and the shallower depth of the embankment in the progressive distance range between about 50 to 80 m are confirmed. Most of the normalized differences among the W/D and LCI models fall within a ±10% range indicating the good correspondence of the two results. The only portions of the section affected by higher positive normalized differences cannot be attributed to errors in the W/D procedure, but to the layering assumption in the LCI. The layered discretization adopted in the LCI can indeed result in an overestimation of the velocity near the layer boundaries (see also Figure 7 for comparison). Most of the higher difference values fall indeed near the embankment/foundation soil interface where the layered profile results from LCI tend to give a sharper transition than the W/D result.

Results of the tomographic inversion of picked first arrivals are reported in Figure 10 and compared, in term of normalized differences, with the Vp results obtained with the W/D procedure. The same equation 1 was adopted for the computation of normalized differences with Vp values

from W/D procedure and first arrivals tomography (these last substituting the LCI values in equation 1).

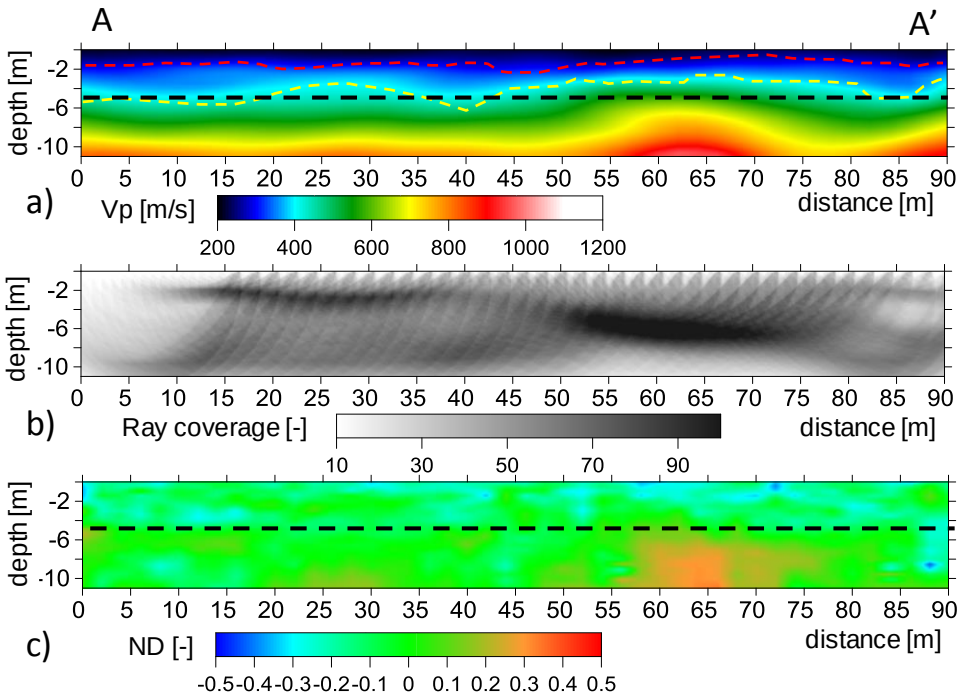

Figure 10 – Results of the first break tomography (section A-A'): a) Vp section, b) Ray coverage along the section and c) Normalized differences with the Vp results of the W/D procedure (colorbars below each figure). On both the sections the supposed depth of the embankment is also reported (dashed black line). Over the tomography the first two interfaces evidenced by the W/D procedure, indicating the transition between the shallow silts and sands (in red), the thickness of the embankment (in yellow), are superimposed.

From Figure 10 it can be observed that, given the reduced length of the streamer adopted, the depth of investigation of the tomography is limited to about 10 m, or even less in some portions. Nevertheless, within this depth, a high ray coverage is obtained in most of the section by the combined elaboration of all the shots. A good convergence of the inversion was obtained with a resulting RMS error of 2.7% after the final iteration.

Again, from Figure 10 it can be observed that the tomographic inversion depicts the same velocity range compared to the one obtained with the W/D procedure. Given the reduced investigation depth of the tomography only the first two interfaces evidenced by the W/D procedure are reported for comparison over the resulting Vp image. Similar variability in the depth of these two interfaces is noted. As an example, both the increased depth of shallower silts and sands around progressive 40 m and the shallower depth of the embankment in the progressive distance range between about 50 to 80 m are confirmed. Being based on relatively long-path raytracing, the tomographic result

shows generally a reduced lateral resolution in the identification of the velocity variations within the section.

Most of the normalized differences, also for Vp, fall within a ±10% range indicating the good correspondence of the two results. The only portion of the section showing higher normalized differences can be attributed to a lower ray coverage zone (see Figure 10b below 7 m at about 55 to 70 progressive distances) making the assumed Vp values less reliable in the tomography. Given its shallower investigation depth, also the tomography does not highlight a marked increase of Vp values, at the bottom of the model, attributable to the presence of the water table.

5. DISCUSSION

It was shown in the paper that the results obtainable with the W/D procedure are comparable both in terms of Vs and Vp to standard seismic processing approaches. This comparison validates therefore the application of the W/D procedure. It was observed, in the presented case study, that most of the normalized differences between the W/D procedure and both LCI and first arrivals tomography fall within a ±10% range, indicating the good correspondence of the two results. Higher normalized differences along the sections can be attributed to different resolution or underlaying methodological assumptions among the methods and cannot be considered as an error in the W/D procedure. A most rigorous validation of the W/D procedure could be obtained through waveform matching from elastic waveform modelling and dispersion comparison. These comparisons were already performed, showing very reliable results, in Khosro Anjom et al. (2019) and Teodor et al. (2020). The Vs and Vp models, from LCI and first arrivals tomography, to which the W/D procedure is here compared are considered standard practice for the seismic characterization. Therefore, the W/D procedure can be established as a reliable alternative to the methods here compared for the characterization of embankments and overall linear earth structures.

The W/D procedure has also main advantages with respect to usually seismic processing approaches applied to the data obtained from similar surveys: i) being a data transform approach it does not requires relevant processing and time consuming interpretations; ii) it does not make any assumption with respect to the number of layers present along the investigated embankment and iii) allow the combined estimation of Vs and Vp for increased depths given the same acquisition setup.

Particularly the first advantage is important if the speed of the surveys is considered, for example in situations in which a fast and preliminary evaluation of the state of health of an embankment is required. This can be the case of surveys conducted after, or in foresee of, significant rain and/or flood events. In these conditions the W/D procedure, applied to the fully automated extracted DCs (Figure 4a), can allow for a first, almost immediate, on site evaluation of the Vs and Vp velocity

field. Both the automated DC extraction step and the conversion of DC data to Vs and Vp profiles is indeed a very fast process (few tens of seconds on a notebook), that outputs direct velocity models while the acquisition is in progress and the streamer is dragged along the embankment.

An example application of this direct visualization of the Vs section during data acquisition is reported in Figure 11. It can be particularly observed that the final Vs section determined from the fully automated extracted DCs (Figure 11d) is roughly comparable with the one determined with the semi-automatic procedure (Figure 8a) with very similar depiction of the main interfaces.

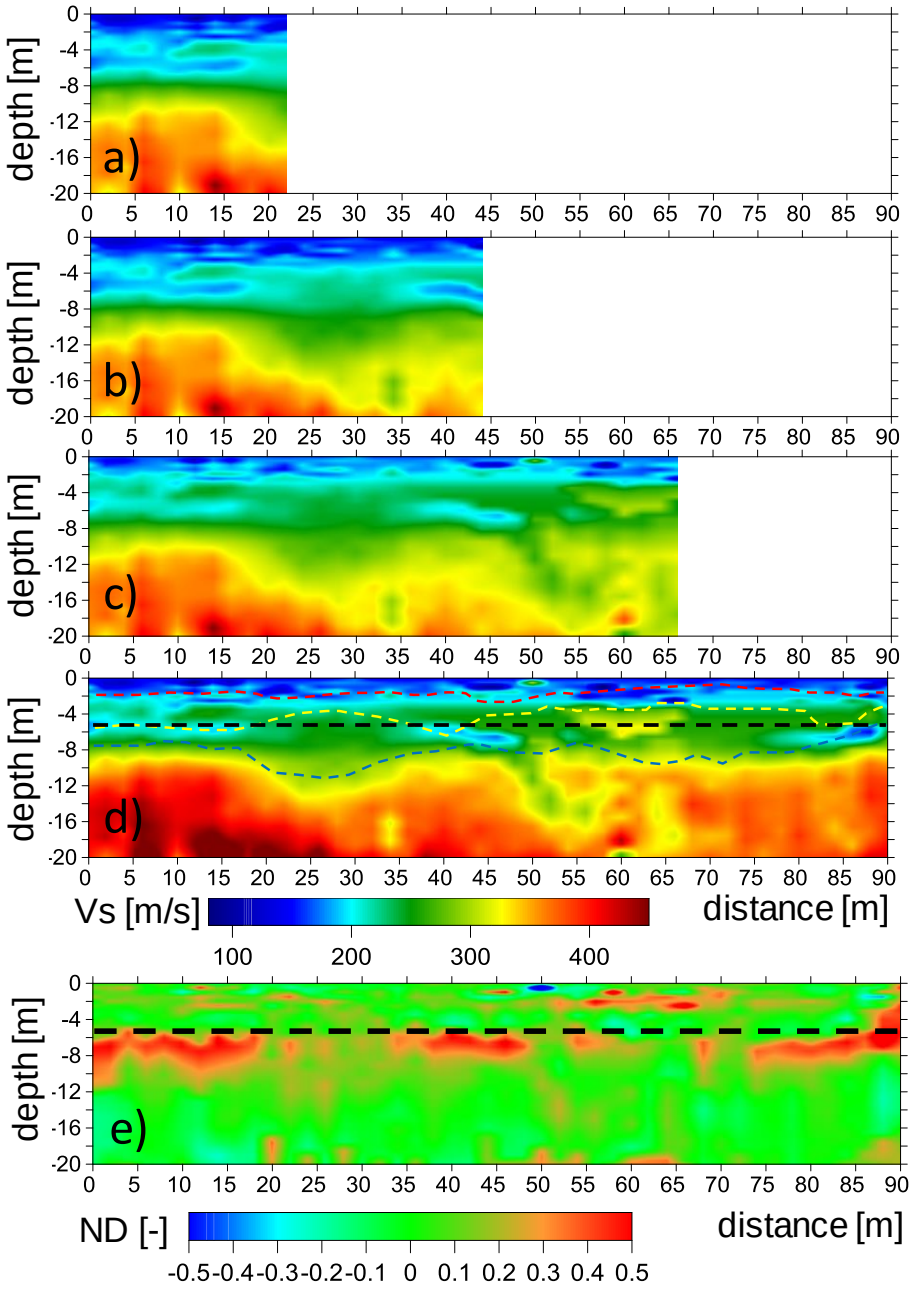

Figure 11 – Example application of the direct visualization of the Vs section during data acquisition: a), b) and c) Vs sections while dragging the streamer along the embankment; d) final Vs section and c) Normalized differences with the LCI (colorbars below each figure). In d) and e) the supposed depth of the embankment is also reported (dashed black line). In d) the interfaces evidenced by the semi-

automated W/D procedure, indicating the transition between the shallow silts and sands (in red), the thickness of the embankment (in yellow) and the transition to compacted gravels and sands (in blue), are superimposed.

The presence of some artefacts can be however noted within the section and can be related to the reduced precision of the automatic picking of the DCs. A general increase in the normalized differences with the LCI (Figure 11d) is also observed, with the presence of localized anomalous local velocity values (e.g. see the shallow portion of the embankment around progressive 50 m). Nevertheless, the general imaging of the Vs structure can be considered accurate enough for a first estimation of the geotechnical variability at the site and a useful tool for a preliminary identification of anomalous portions of the examined embankments. Given the use of the same Poisson ratio profile (Figure 8c), uniform through the section, very similar considerations can be performed for what concerns the resulting Vp image.

This direct visualization requires the knowledge of reference Vs and Vs,z profiles over which calibrate the W/D relationship and the following Poisson ratio computation. In the present paper these reference profiles where obtained through MCI of a reference DC. The same approach can be adopted on site at the beginning of the surveys by selecting one of the clearer DCs during the first shots. Nevertheless, the MCI step can be significantly time consuming and not always applied with reliability on site. Possible alternative approaches would therefore require the execution of initial detailed tests and interpretations through which determine with accuracy the reference profiles and only later proceed with the execution of the streamer surveys. Alternatively, the reference profiles can be extracted form already available geotechnical and/or geophysical surveys along the embankment. With this respect the W/D procedure already showed comparable results also with respect to Down Hole surveys (Socco et al., 2017).

In both the automatic and semi-automatic procedures, the DCs uncertainties in the maxima identifications were not considered (Figure 4). This is in-line with the aim of obtaining a fast imaging tool for the seismic properties of the studied embankment. A rigorous experimental uncertainties evaluation requires indeed a statistical population of test repetitions (i.e., multiple shots at different locations) which could compromise the speed of the surveys. Alternative uncertainties estimations can be attempted with a single seismic shot by considering, for each frequency, the phase velocities whose energy maxima fall within a certain range of the of picked one. These last uncertainties are a partial estimation of the true ones, since reflect the intrinsic resolution of the geometrical arrangement adopted in acquisition, but could be worth considered in future developments of the methodology. If experimental uncertainties are correctly estimated their

propagation to the final velocity models can be obtained as performed by Khosro Anjom et al. (2019).

Limitations of the proposed W/D procedure can be related to: i) its application to only fundamental mode DC; ii) the assumption of a laterally invariable W/D relationship and Poisson ratio along the embankment. With respect to the first one, the W/D procedure has been mainly developed and applied to fundamental mode DC, but some attempts have been already made to include also higher propagation modes (e.g. Bamarouf et al., 2017). Including higher modes showed to give advantages mainly with respect to the investigation depth, even dough it is a more time-consuming process. However, this could be a necessary step along embankments with peculiar shape dimensions, since it is well known that the shape of the embankment could influence the surface wave dispersive pattern and modes superposition (e.g. Karl et al., 2011). Pageot et al. (2016) have also shown that internal structure layering can emphasize geometrical effects and produce DCs very different from the theoretical 1D case, for both the fundamental and higher modes. In these conditions even a multi-modal inversion approach could encounter some limitations to infer accurate Vs and Vp models.

These effects have not been particularly noted at the site. As it can be observed in Figure 3b, higher modes are indeed present in the higher frequency range, but the fundamental mode propagation is still easily recognizable as local energy maxima. This may be related to the reduced contrast between the embankment body and the underlaying subsoil (Figure 2) which limits the layering effect and to the relevant width of the embankment (width to height ratio of about 5.5) which limits the presence of 3D effects.

Conversely the laterally invariant assumption could be easily overcome using appropriate clustering techniques on the extracted DCs that can be analysed for grouping them into subsets with homogeneous properties. The W/D procedure has then to be applied to each of the identified subsets. The application of this further processing step however increases again the computation times and prevent a direct in situ application of the procedure but has been shown to provide increased resolution in the identification of sharp lateral variations with the W/D procedure (Khosro Anjom et al., 2019; Teodor et al., 2020).

The clustering approach was judged to be unnecessary in the presented case study given the uniformity of the extracted DCs (see Figure 4) which suggest the presence of smooth depth variations along the embankment but the absence of particularly sharp variations. When sharp lateral variations along the embankment are the main survey target alternative identification methods based on the surface waves spectral properties (e.g. Colombero et al., 2019) could also be applied to the acquired streamer data.

To allow for a more complete characterization of the state of health of embankments, seismic data are usually combined with electric resistivity data. These last can indeed give important information on the variations of soil composition and water saturation, detect development of weak zones and identify local anomalies potentially related to seepage. The combined use of seismic and electrical data can indeed provide an effective geotechnical characterization of these earth structures, as shown by several research groups that are working on their integration (e.g. Takahashi et al., 2014; Goff et al. 2015; Lorenzo et al., 2016). In this respect the W/D procedure has its natural development in combination with mobile electric systems allowing also a fast and effective evaluation of resistivity properties (e.g. Kuras et al., 2007; Comina et al., 2020).

6. CONCLUSION

This paper presents the application of a novel processing approach (W/D procedure) to surface wave streamer data. This approach is based on the definition a wavelength/depth (W/D) relationship for surface waves and allows the combined definition of shear (Vs) and compressional (Vp) wave velocities. The results obtained within the paper with the W/D procedure are comparable to standard seismic processing approaches with the advantage of reduced survey time and increased efficiency. It was shown in the paper as the W/D procedure can be developed in order to be completely automated and used as a fast in situ imaging tool along embankments for preliminary evaluations on their state of life.

Processing of the seismic streamer data yielded to an effective characterization of the Vs and Vp velocity field along the studied embankment. The origin and properties of the anomalies encountered could be better studied with the use of local geotechnical investigations to provide a more specific knowledge on the state of life of the embankment. The produced seismic sections, if properly calibrated with the few independent geotechnical tests available, can be nevertheless used for preliminary stability evaluations also in portion of the embankment non directly covered by geotechnical tests.

Further studies, already planned and partially executed, include the application of the W/D procedure to different embankments shapes with the eventual inclusion of higher modes in the interpretation. Moreover, the combined acquisition of electrical resistivity data, even with innovative acquisition approaches, will allow the contemporary execution of resistivity and seismic surveys with even more reduced survey time and increased knowledge on the state of health of the embankments due to the acquisition of the different complementary parameters.

ACKNOWLEDGMENTS

This work has been funded by FINPIEMONTE within the POR FESR 14/20 "Poli di Innovazione - Agenda Strategica di Ricerca 2016 - Linea B" call for the project Mon.A.L.I.S.A. (313-67). Authors thank Daniele Negri for helping during acquisition surveys. Authors are thankful to the two anonymous reviewers whose comments helped in improving the work.

REFERENCES

1. Arato A., Naldi M., Vai L., Chiappone A., Vagnon F. and Comina C. (2020) Towards a Seismo-Electric land streamer, submitted for the 6th International Conference on Geotechnical and Geophysical Site Characterization, 7-11 September 2020, Budapest.
2. Auken, E., and A. V. Christiansen, 2004, Layered and laterally constrained 2D inversion of resistivity data: Geophysics, 69, 752–761.
3. Bamarouf, T., Socco, L.V. & Comina, C., 2017. Direct Statics estimation from ground roll data—the role of higher modes, in 79th EAGE Conference and Exhibition.
4. Bergamo P, Dashwood B, Uhlemann S, Swift Chambers JE, Gunn DA, Donohue S (2016) Time-lapse monitoring of fluid-induced geophysical property variations within an unstable earthwork using P-wave refraction. Geophysics 81(4):17–27
5. Bièvre, G., Lacroix, P., Oxarango, L., Goutaland, D., Monnot, G., Fargier, Y., 2017. Integration of geotechnical and geophysical techniques for the characterization of a small earth-filled canal dyke and the localization of water leakage. J. Appl. Geophys. 139, 1–15.
6. Boore, D., 2007, Dave Boore's notes on Poisson's ratio (the relation between VP and VS), http://www.daveboore.com/daves_notes.html, accessed 03 March 2017.
7. Busato, L., Boaga, J., Peruzzo, L., Himi, M., Cola, S., Bersan, S., Cassiani, G., 2016. Combined geophysical surveys for the characterization of a reconstructed river embankment. Eng. Geol. 211, 74–84.
8. Chao C et al (2006) Integrated geophysical techniques in detecting hidden dangers in river embankments. J Environ Eng Geophys 11:83–94.
9. Colombero, C., Comina, C., Socco, L.V. (2019) Imaging near-surface sharp lateral variations with surface-wave methods - Part 1: Detection and location, Geophysics, 84 (6), pp. EN93-EN111.
10. Comina C., Vagnon F., Arato A., Fantini F. and Naldi M., Application of a new electric streamer to the characterization of river embankments, submitted to Journal of Geotechnical and Geoenvironmental engineering.
11. Dal Moro G., M. Pipan, E. Forte and I. Finetti, 2005, Determination of Rayleigh wave dispersion curves for near surface applications in unconsolidated sediments, SEG Technical Program Expanded Abstracts 2003, pages 1247-1250.
12. Foti, S., Lai, C.G., Rix, G.J., Strobbia, C., 2014. Surface Wave Methods for Near-Surface Site Characterization. CRC Press.
13. Goff, D.S., Lorenzo, J.M., Hayashi, K. "Resistivity and shear wave velocity as a predictive tool of sediment type in coastal levee foundation soils, 28th Symposium on the Ap-plication of Geophysics to Engineering and environmental Problems 2015, SAGEEP 2015, pp. 145-154.
14. Hu Hao, Mustafa Senkaya, Yingcai Zheng, A novel measurement of the surface wave dispersion with high and adjustable resolution: Multi-channel nonlinear signal comparison, Journal of Applied Geophysics, Volume 160, 2019, Pages 236-241.
15. Karl, L., Fechner, T., Schevenels, M., François, S., Degrande, G., 2011. Geotechnical characterization of a river dyke by surface waves. Surf. Geophys. 9, 515–527.
16. Khosro Anjom, F., D. Teodor, C. Comina, R. Brossier, J. Virieux, and L. V. Socco, 2019, Full waveform matching of Vp and Vs models from surface waves, Geophysical Journal International, 218, 1873-1891.
17. Kramer S.L. 1996. Geotechnical Earthquake Engineering. Prentice Hall.
18. Kuras, O., Meldrum, P.I., Beamish, D., Ogilvy, R.D., Lala, D. "Capacitive resistivity imaging with towed arrays", 2007, Journal of Environmental and Engineering Geophysics, 12 (3), pp. 267-279.

19. Lane Jr. J.W., Ivanov J., Day-Lewis F.D., Clemens D., Patev R. and Miller R.D. 2008. Levee evaluation using MASW: Preliminary findings from the Citrus Lakefront Levee, New Orleans, Louisiana. 21st Symposium on the Application of Geophysics to Engineering and Environmental Problems, Philadelphia, USA, Expanded Abstracts, 703–712.
20. Li Jing, Zongcai Feng, Gerard Schuster, Wave-equation dispersion inversion, Geophysical Journal International, Volume 208, Issue 3, 1 March 2017, Pages 1567–1578.
21. Lorenzo, J.M., Goff, D.S., Hayashi, K. "Soil-Type estimation beneath a coastal protection levee, using resistivity and shear wave velocity" 22nd European Meeting of Environ-mental and Engineering Geophysics, Near Surface Geoscience 2016.
22. Lutz K., Fechner T., Schevenels M., Stijn F. and Degrande G., 2011, Geotechnical characterization of a river dyke by surface waves, Near Surface Geophysics, Volume9, Issue6, Pages 515-527.
23. Min D.-J. and Kim H.-S. 2006. Feasibility of the surface-wave method for the assessment of physical properties of a dam using numerical analysis. Journal of Applied Geophysics 59, 236–243.
24. Pageot, D., Le Feuvre, M., Donatienne, L., Philippe, C., Yann, C., 2016. Importance of a 3D forward modeling tool for surface wave analysis methods, in: EGU General Assembly Conference Abstracts. p. 11812.
25. Pan Yudi, Lingli Gao, Renat Shigapov, Multi-objective waveform inversion of shallow seismic wavefields, Geophysical Journal International, Volume 220, Issue 3, March 2020, Pages 1619–1631.
26. Park, C. B., Xia, J., and Miller, R. D., 1998, Imaging dispersion curves of surface waves on multichannel record: 68th Ann. Internat. Mtg., Soc. Explor. Geophys., Expanded Abstracts, 1377-1380.
27. Rahimi S., Clinton M. Wood, Folaseye Coker, Timothy Moody, Michelle Bernhardt-Barry, Behdad Mofarraj Kouchaki, 2018, The combined use of MASW and resistivity surveys for levee assessment: A case study of the Melvin Price Reach of the Wood River Levee, Engineering Geology, Volume 241, Pages 11-24.
28. Samui, P., Sitharam, T.G. Correlation between SPT, CPT and MASW (2010) International Journal of Geotechnical Engineering, 4 (2), pp. 279-288.
29. Samyn, K., Mathieu, F., Bitri, A., Nachbaur, A., Closset, L., 2014. Integrated geophysical approach in assessing karst presence and sinkhole susceptibility along flood-protection dykes of the Loire River, Orléans, France. Eng. Geol. 183, 170–184.
30. Sentenac P, Benes V, Keenan H (2018) Reservoir assessment using non-invasive geophysical techniques. Environmental Earth Sciences 77(293):1-14
31. Socco, L.V. and Boiero, D., 2008. Improved Monte Carlo inversion of surface wave data, Geophys. Prospect., 56, 357–371.
32. Socco, L. V., D. Boiero, S. Foti, and R. Wisén, 2009, Laterally constrained inversion of ground roll from seismic reflection records: Geophysics, 74, no. 6, G35–G45.
33. Socco, L. V., and C. Comina, 2015, Approximate direct estimate of S-wave velocity model from surface wave dispersion curves: 21st Annual International Conference and Exhibition, EAGE, Extended Abstracts, A09.
34. Socco, L.V., Comina, C. and Khosro Anjom, F., 2017. Time-average velocity estimation through surface-wave analysis: Part 1—S-wave velocity, Geophysics, 82(3), U49–U59.
35. Socco, L.V. and Comina, C., 2017. Time-average velocity estimation through surface-wave analysis: Part 2—P-wave velocity, Geophysics, 82(3), U61–U73.
36. Takahashi T, Yamamoto T (2010) An attempt at soil profiling on a river embankment using geophysical data. Explor Geophys 41(1):102–108
37. Takahashi, T., Aizawa, T., Murata, K., Nishio, H., Mat-suoka, T. "Soil permeability profiling on a river embankment using integrated geophysical data", 2014, SEG Technical Program Expanded Abstracts, 33, pp. 4534-4538.
38. Teodor D., Comina C., Khosro Anjom F., Socco L.V., Brossier R. and Virieux J., 2020, Challenges in shallow targets reconstruction by 3D elastic full-waveform inversion – Which initial model?, submitted to Geophysics.